Journal of Applied Polymer Science

Fabrication of hierarchical wrinkled morphologies through sequential UVO treatments

Juan Rodríguez-Hernández,[1] Adolfo del Campo[2]
[1]Instituto de Ciencia y Tecnología de Polímeros (ICTP-CSIC), C/Juan de la Cierva 3, 28006 Madrid, Spain
[2]Instituto de Cerámica y Vidrio (ICV-CSIC), C/Kelsen 5, 28049-Madrid, Spain
Correspondence to: J. Rodríguez-Hernández (E-mail: jrodriguez@ictp.csic.es)

ABSTRACT: The fabrication, in a controlled manner, of well-defined micrometer size topographical features on polymer surfaces is a great challenge due to the large variety of potential applications of these materials ranging from adhesion, optics to responsive interfaces. A challenging issue concerns the fabrication of interfaces having surface moieties with sizes at different length scales. Herein we describe the fabrication of hierarchical wrinkled surfaces involving two sequential ultraviolet-ozone (UVO) treatments. This methodology allowed us to tailor the shape of PDMS surfaces and create a large variety of different patterns expected to have a broad range of applications requiring surface features with variable sizes. More interestingly, the employment of UVO treatments to produce surfaces with up to three distinct levels of order since they enable the rigidification of the interface by formation of a SiO_x layer or the degradation of the PDMS surface when longer treatments. The surfaces prepared by using this approach presented patterns three different scales: the structure provided by the mask employed, the wrinkled surface inside of the directly exposed areas (related to the hole size of the mask) and the wrinkled surface protected during the first treatment by the mask (which is related to the mesh dimensions of the mask employed). © 2015 Wiley Periodicals, Inc. J. Appl. Polym. Sci. **2015**, *132*, 41863.

KEYWORDS: coatings; degradation; morphology; surfaces and interfaces

Received 22 September 2014; accepted 10 December 2014
DOI: 10.1002/app.41863

INTRODUCTION

Patterning polymer surfaces with well-defined topographical features is a rapidly expanding research area since the final use of a particular polymeric material largely relies on their surface micro and nanostructure. In particular, wrinkling on soft polymeric substrates is one of the patterning approaches that have become an increasing attention during the last decade. This is a consequence of the multiple applications found for these structured interfaces. Among others, wrinkled interfaces have been employed for the preparation of stretchable electronics,[1–4] as templates to induce nanoparticle ordering[5–8] or to obtain surface with anisotropic and/or tunable wettability.[9] These surfaces are also of highly interest in the preparation of materials with surfaces having variable adhesion/friction[10–13] or provided the length scale of the wrinkles is in the range of the visible for their photonic applications.[9,14–17]

Wrinkles are produced on elastic polymers when an induced mechanical instability (stretching, compression) is accomplished first by the formation of a rigid interface. In the most extended case a polymer support is mechanically stretched and a surface treatment is applied on the top surface. Among the surface treatments to obtain a stiff interface, UV-irradiation, ozone exposure or the deposition of rigid layers (metallic or polymeric) are the most extended.[18–26] Finally, upon release of the mechanical force an out of plane deformation is produced thus leading to buckling. Surface wrinkling exhibit several major advantages compared to other patterning approaches including its spontaneous nature, its versatility or its ability to generate large area patterns without requiring expensive lithographic techniques.[27–32]

Since the pioneer experiments carried out among others by Whitesides and coworkers[33] to control the preparation of wrinkles large number of studies and reviews have been devoted to this patterning approach. Initially, the patterns obtained using surface wrinkles were limited either to random structures or in the case of wrinkles formed by mechanical stresses to surface wrinkles generally aligned perpendicular to the direction of the applied force.[18,34–36]

However, the preparation of more complex or even hierarchically ordered wrinkled surfaces, i.e. ordered surface patterns at different length scales have been pursued motivated by the extraordinary properties they exhibit.[37] Spontaneous wrinkling of a rigid membrane (a metal layer, a polymer coating or obtained upon surface treatment) on a soft foundation (elastic

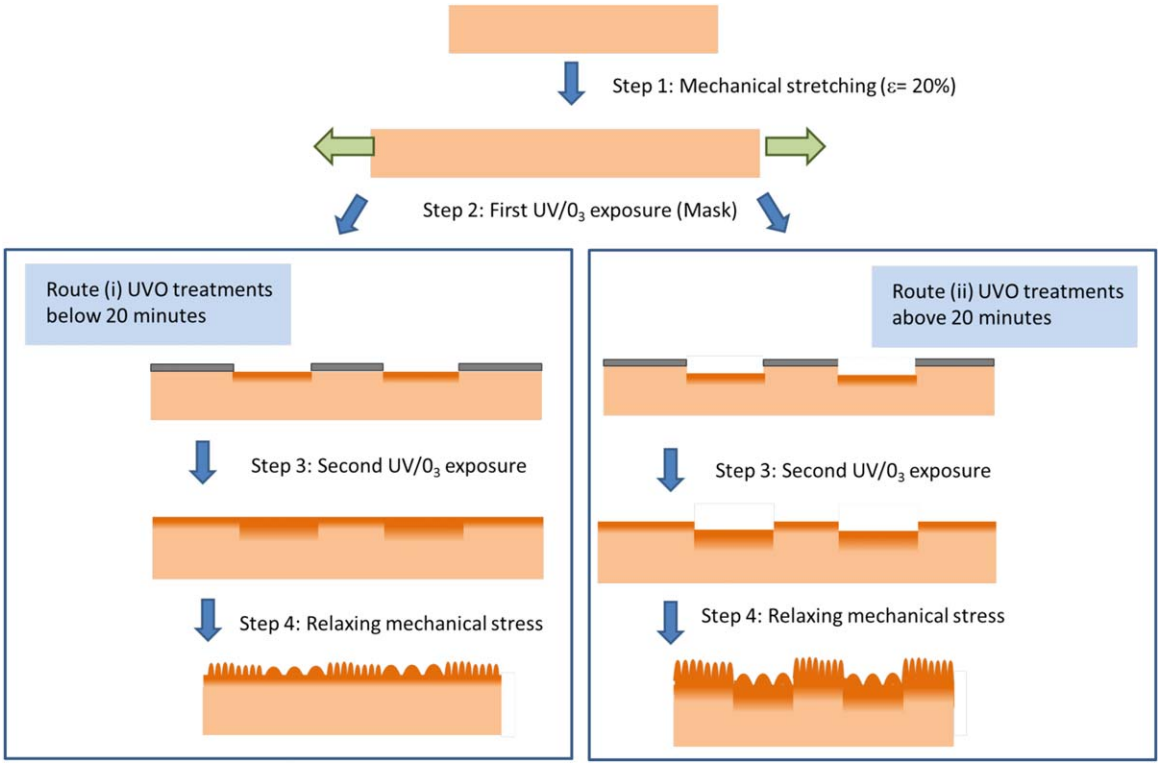

Figure 1. Scheme for hierarchical wrinkle formation upon two consecutive UVO treatments using during the first UVO exposure a mask. Whereas short irradiation times (i) produced planar surfaces with variable wrinkle dimensions, longer UVO treatments produced additionally surface degradation and permit the fabrication of surfaces with surface topography (ii). [Color figure can be viewed in the online issue, which is available at wileyonlinelibrary.com.]

polymer layer) has been employed by different ways to prepare complex features[36,38–41] with gradually variable topographies ranging from the nano- to the microscale.[18,33,42–46] However, most of these structures require the use of several steps and require the combination of different patterning methods. For instance, hierarchically structured PDMS have been recently fabricated by following a two-step procedure.[9] First, the PDMS prepolymer mixture is poured over the patterned anodic aluminium oxide (AAO) template and cured. After peeling off from the template a nanopillar structured PDMS film was then uniaxially stretched and exposed to ultraviolet-ozone (UVO) radiation. Upon releasing the strain, in addition to the nanopillars wrinkled microstructures were obtained. Both nanopillars aspect ratio and the wrinkle dimensions can be varied. Moreover, stretching the wrinkled film back to the initial strain removed the microscale structure, and only the nanopillar array structure remained. Other groups are also currently involved in the fabrication of hierarchically ordered surface wrinkled patterns by using different approaches for instance using molds[42,47] controlling the diffusion front[44] or by fabricating multilayers on stretched PDMS.[45]

Within this context and in a dynamic research field that seek for alternatives to control the surface topography, herein we propose a simple approach to create hierarchically structured wrinkled structures based on the simultaneously occurring rigidification/degradation processes by using UV/O_3. As will be depicted below, based on this surface treatment we obtained hierarchically structured interfaces exhibiting surface moieties with three different levels of order that can be modulated. Moreover, UVO treatments can equally produce the degradation of polymeric materials. Hence, the control over the rigidification-degradation kinetics allowed us to introduce additional surface features by using PDMS as elastic foundation.

RESULTS AND DISCUSSION

The oxidation of the PDMS surface with UVO transformed the top surface of the PDMS into a rigid silicate-like layer while below, the elastic properties remains invariable. As has been already depicted in the literature, the time of exposure to these oxidative conditions alters not only the modulus of the PDMS surface but also the thickness of the silica layer originated which is dependent on the exposure time.[48–51] As a consequence, depending on the exposure different wrinkle characteristics, i.e., variable period and amplitude can be obtained. Thus, in principle, provided the control over the areas exposed, the UVO treatment will permit to precise define areas with larger and shorter exposure times and therefore produce variable wrinkle dimensions at particular surface positions. Moreover, UVO treatments are generally employed to activate inorganic surfaces, to functionalize with hydrophilic functional groups organic surfaces but also to remove organic contaminants from inorganic supports. In effect, UVO treatments are capable of decomposing organic material upon an appropriate intensity. Based on these two concepts, i.e., the possibility of

controlling the distribution of the UVO treatment using, for instance, a copper TEM grid as a mask and knowing that depending on the duration of the UVO exposure we can modify the surface pattern we will be able to fabricate surfaces with variable degree of structuration.

The strategy employed to produce wrinkles with controlled dimensions and shape is depicted in Figure 1 Route (i). The films prepared using Sylgard 184 were stretched to a 20%. Then a particular mask (in this case a square or a hexagonal shaped grid template) is placed on top of the stretched surface. A first UVO treatment transforms the exposed surface areas of PDMS into rigid silica while the non-exposed areas covered by the mask remain protected were not modified. Upon removal of the mask, a second UVO treatment was applied. As a consequence of these two treatments, the surfaces have discrete areas defined by the mask employed with two different thicknesses of silica layer. Upon relaxation of the stress applied we expect, thus, the surface to buckle and thus produces surface with variable wrinkle dimensions.

The formation of SiO_x during the UVO treatments has been followed by IR and/or contact angle (CA) measurements. On the one hand, the surface water CA measured in samples irradiated during 20 min exhibit total wetting and, therefore, confirmed the formation of a hydrophilic layers upon surface oxidation.[49] On the other hand, IR confirmed a decrease of in the —CH_3 signals (bands 785–815 cm^{-1}, 1245–1270 cm^{-1} and 2950–2970 cm^{-1}) that is accompanied by an increase in —OH signal (bands 825–865 cm^{-1}, 875–920 cm^{-1}, and 3050–3700 cm^{-1}), suggesting oxidative conversion of the —[$(CH_3)_2$Si—O]— molecules into more hydrophilic species.[49] Both techniques deliver information that permits the surface description of the consequences of the UVO treatment. Whereas, both methods provide information about the increase of the surface hydrophilicity and the variations on the chemical composition, they do not permitted us to follow the changes on the distribution of the surface chemical variations with micrometer size lateral resolution. To obtain this information, we employed confocal Raman microspectroscopy integrated with atomic force microscopy (AFM). In particular, we have analyzed the raman spectra of samples irradiated using mask at different times in the areas directly exposed and those protected by the mask. For comparative purposes we additionally carried out the analysis of a sample that has been exposed 10 min using a mask and also to a second UVO treatment without the mask. In Figure 2, the spectra of a non irradiated sample and a sample exposed to UVO during 30 min using a hexagonal mask are depicted. In this spectra, we observed a band at 1174 cm^{-1} (Band I) that increases during the irradiation process and the band at 1270 cm^{-1} (Band II) that remains constant during the treatment. These two signals were employed to follow the surface treatment as a function of time. The image included in Figure 2 has been constructed by merging the maps of the different components: blue regions represent the higher intensity for the 1174 cm^{-1} associated with the modified PDMS while the red color areas correspond to a low intensity of the same signal (non-modified PDMS). This image indicates that the areas non-protected by the mask have been selectively modified.

To follow the kinetics of the surface modification Raman spectra have been recorded at different irradiation times. Figure 3 shows the Raman spectra containing Band I and Band II employed for the analysis of the surface modification of the PDMS. As has been depicted for the treatments from 0 to 30 min (A) to (D), the areas below the mask (i) exhibit the same Raman spectra indicating that the surface remains intact after the treatment. On the contrary, the areas exposed (ii) have been gradually modified as evidenced by the systematic increase from (A) to (D) of the signal intensity of Band I. Figure 3 additionally shows the Raman spectra obtained for a sample treated 10 min with the mask and 10 additional minutes without the mask (E). In this case, we observed an increase of the Band I both inside and outside the pattern defined by the mask. Nevertheless, the intensity of the signal inside the hexagonal holes of the mask is larger in comparison to the intensity of the signal in the areas protected during the first 10 min of treatment. This behavior is clearly shown in Figure 3(iii) where the ratio of Band I and Band II is represented for each treatment both for areas below the mask (black) and those directly exposed (red). It is important to note that the ratio in sample (E) is larger than the expected for the same exposure time, i.e., 20 min (sample B). Most probably the O_3 flow is somehow reduced in

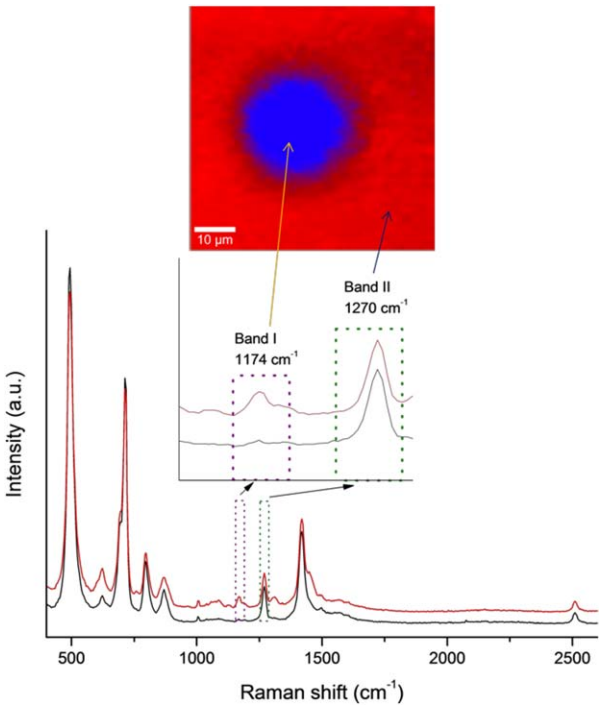

Figure 2. Raman confocal analysis of the samples irradiated with a hexagonal mask. Band I increases during the UVO treatment while Band II remains constant. These two bands can be employed to follow the extent of the chemical surface modification. The image included correspond to a Raman micrographs constructed by merging the maps of the different components: blue regions represent the higher intensity for the 1174 cm^{-1} associated with the modified PDMS while the red color areas correspond to a low intensity of the same signal (non-modified PDMS). [Color figure can be viewed in the online issue, which is available at wileyonlinelibrary.com.]

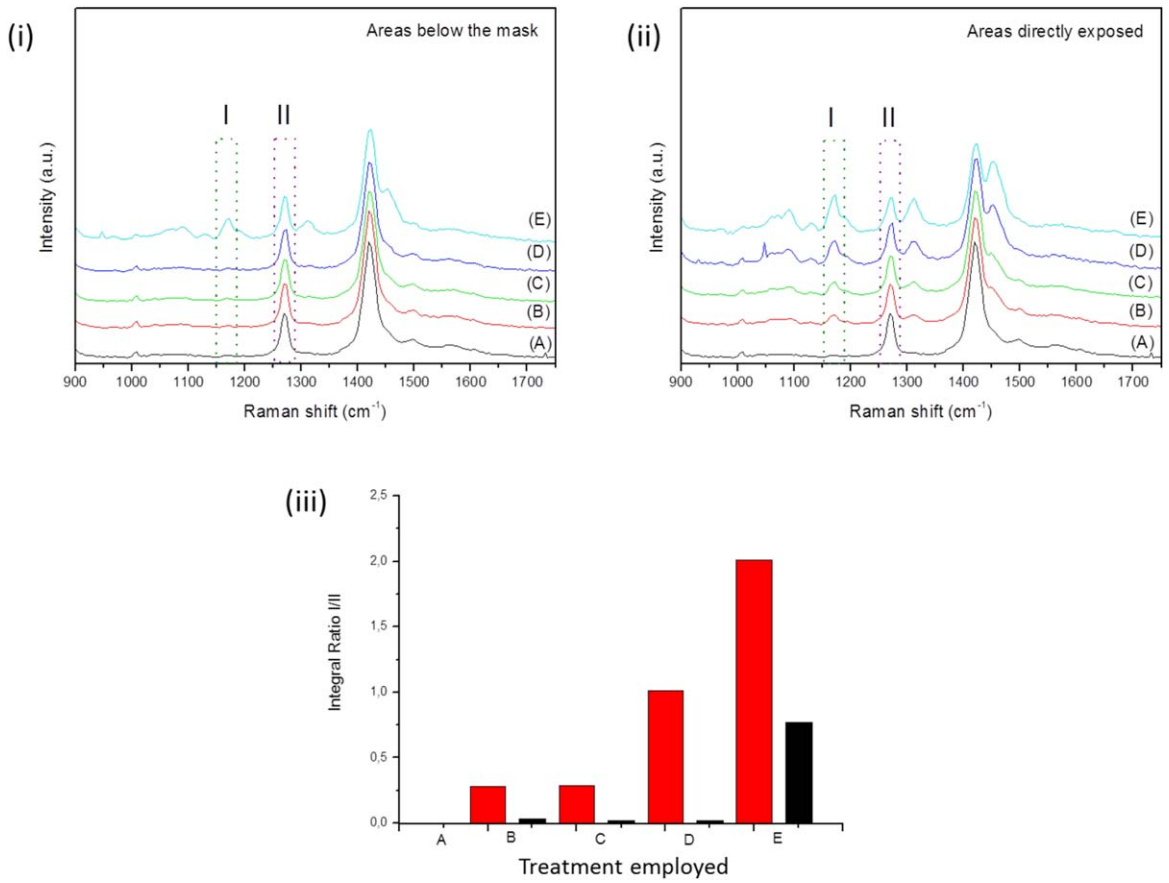

Figure 3. (i) Raman spectra of the samples in the areas protected by the mask during the UVO treatment as a function of time, (ii) Raman spectra of the samples in the areas directly exposed to the UVO treatment as a function of time. The samples were exposed (A) 0 min, (B) 10 min, (C) 20 min, (D) 30 min, and (E) 10 min with mask and 10 min upon removal of the mask. (iii) Variation of the signal intensity ratio Band I/Band II in the areas directly exposed to UVO (red) and those protected by the mask (black). [Color figure can be viewed in the online issue, which is available at wileyonlinelibrary.com.]

the vicinity of the surface as a consequence of the mask employed that has a thickness of ~30 μm.

Upon evidencing the different of the surface chemical modification as a function of the duration of the treatment we prepared the wrinkled interfaces by using the two-step procedure depicted in Figure 1(i). In Figure 4, are depicted the SEM images of the wrinkles obtained using a 400 Mesh TEM grid (Hole Width 37 μm; Bar Width 25 μm). We have initially limited the exposure time to study the influence of the SiO_x thickness originated at the surface on the wrinkle characteristics obtained. The treatments employed for this series of experiments were limited to either 10 or 20 min using the mask and 10 or 20 min upon removal of the mask. It has to be mention at this point that both steps are required to obtain such morphologies. The removal of step 3 (Figure 1) in the procedure did not produced the formation of wrinkles. The selective rigidification of the surface allows the areas that were not exposed during this treatment to remain elastic. Therefore, upon removal of the stretching applied these areas are able to dissipate the compressive energy created by the stiffness of the exposed areas.

Several important observations can be extracted from Figure 3. First, the duration of the first treatment is directly related to the size of the wrinkles of the exposed areas. Thus, by comparison of (a) and (c) a clear increase of the wrinkle size from $5.2 \pm 0.5\times$ μm to 7.1 ± 0.6 μm can be observed. As has been previously reported, during UVO exposure a rigid film is progressively formed and can be of 10–12 nm in thickness after 10 min and ~15 nm after 20 min. The growth in thickness of the stiff silica layer resulted in an increase of the wrinkle characteristics.[48] It has to be mentioned at this point that shorter treatments did not form any wrinkle in these areas. Most probably the SiO_x layer formed is too thin and therefore possesses a limited stiffness required to induce the out of plane deformation.

Wrinkle characteristics of the exposed areas did not exhibit significant changes between the sample (a) and (b) that were treated 10 min in step 2. However, the wrinkle characteristics of the non-exposed areas significantly changed. Sample (a) exhibit rather long and straight wrinkles connecting the areas exposed during the two steps with $\sim 3.7 \pm 0.4$ μm in size. Sample (b) presented a rather disordered wrinkled structure with smaller wrinkle sizes 3.2 ± 0.3 μm. In summary, we can conclude that, as a result of the variation of the UVO exposure time and the pattern of the mask employed, we are able to form buckled interfaces with variable wrinkle characteristics.

In addition to the variation of the surface pattern depending on the duration of the UVO treatment we additionally take

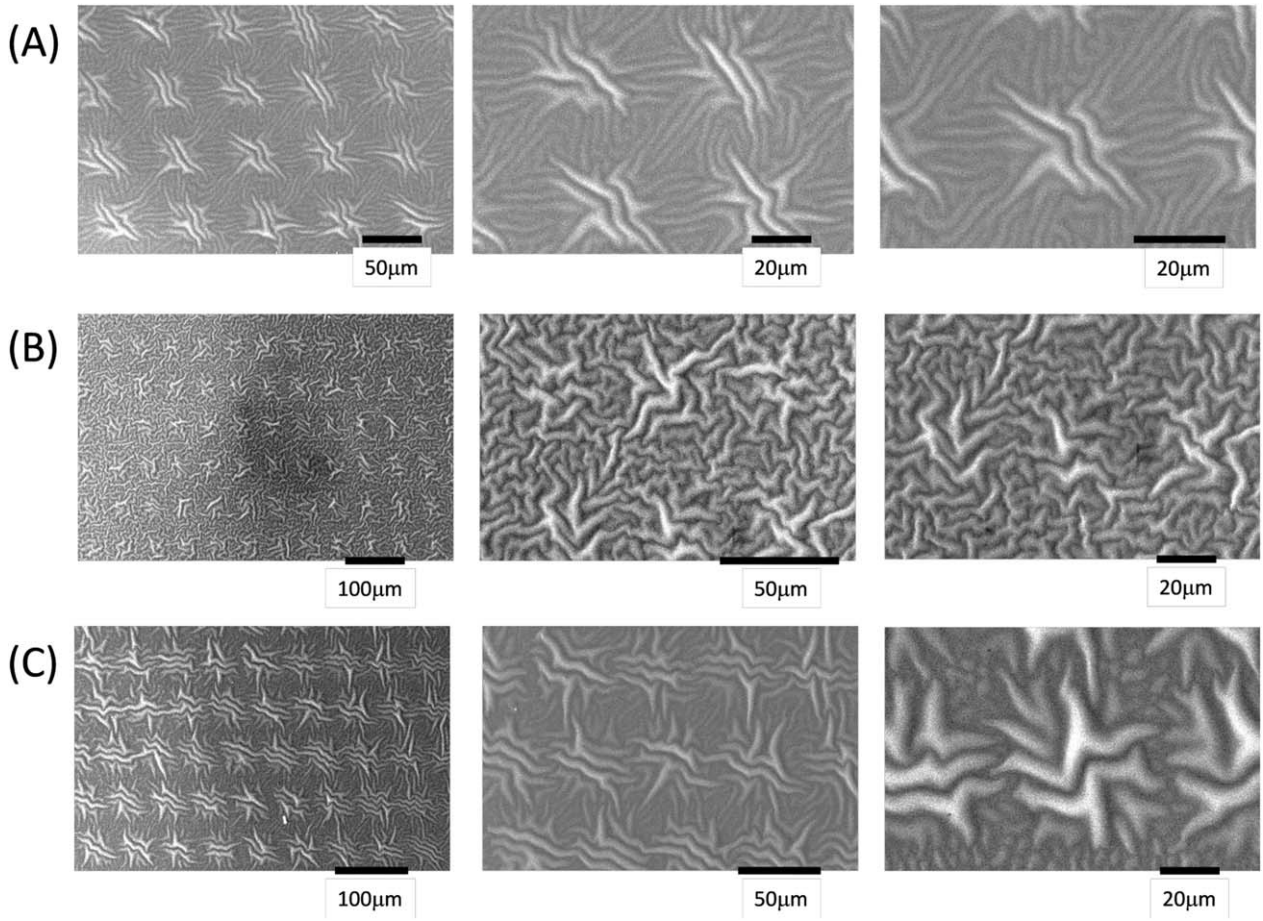

Figure 4. SEM images of wrinkled surface obtained using this approach varying the exposure time of step 2 and step 3. (A) Step 2: 10 min. Step 3: 10 min, (B) Step 2: 10 min. Step 3: 30 min and (C) Step 2: 20 min. Step 3: 10 min.

advantage of the partial degradation of the PDMS occurring for longer UVO treatments [Figure 1—Route (ii)]. Based on these concurrent processes (rigidification/degradation) we are able to fabricate wrinkled surface with variable morphologies and wrinkle dimensions and induce an additional surface topography depending on the features of the mask employed. In this case, the topographical variations are not only due to the out of plane deformations that leads to wrinkle formation but also to a partial surface degradation. It is already known that extensive UVO treatments degrade most organic materials and this treatment has been typically employed to remove organic rests from inorganic surfaces. UVO treatments have been also extensively employed to functionalize organic materials.[52,53] Nevertheless, the capability of UVO treatments to pattern organic polymer films has not been exploited up to date. In the case of PDMS, it has been reported that UVO converts polysiloxanes to SiO_x upon relative short exposure times. However, larger treatments produces a loss in mass as a consequence of the removal of small organic molecules resulting of the surface decomposition.[48] Taking advantage of this second process, we exposed the PDMS film to UVO during different times using a mask to distinguish between exposed and non-exposed areas. In this particular case, as depicted in Figure 5, we used a hexagonal patterned mask. By means of an optical profilometer, we evaluated the effect of longer UVO treatments on the surface morphology and studied the induced topography. As depicted in Figure 5, the UVO degradation on the directly exposed areas induces the formation of cavities with a hexagonal morphology. Moreover, the depth of the structures varied as a function of the treatment employed. Whereas at short irradiation times below 20 min a diffuse surface pattern is observed an increase of the exposure time leads to a well-resolved surface pattern exhibiting an step between exposed and non-exposed areas up to 1.2 μm for a treatment during 2 h (Figure 5). It has to be mentioned that longer treatments (up to 4 h) did not significantly improve the step obtained and appears to be a self-limiting process.[48]

According to Efimenko *et al.*[49] UVO treatments as long as 60 or 90 min lead to a hydrophilic SiO_x layer of 60–70 nm. In view of the results mentioned above, i.e., the steps observed for these treatments are close to 1 μm, we can conclude that the pattern observed is not only due to a mass reduction resulting from the density decrease and collapse during the formation of SiO_x which has been estimated to be 50%.[54] Apart from the constant chemical transformation occurring at the extreme surface (50–70 nm) an extensive UVO treatment is able to remove the surface top layer by degradation. Therefore, upon removal of the

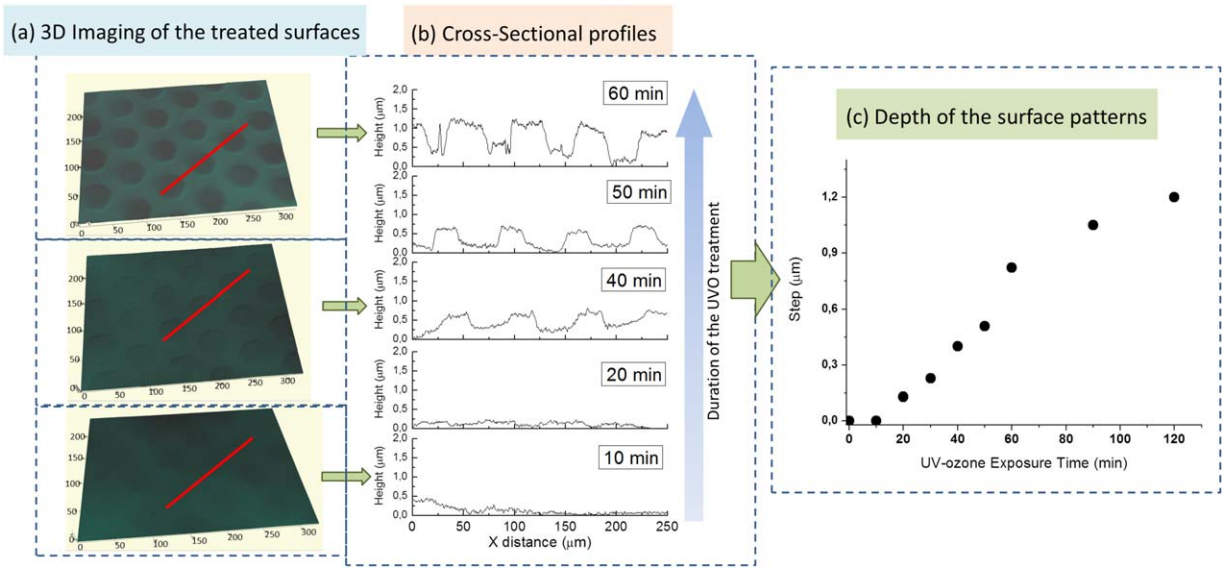

Figure 5. Left: 3D images of PDMS surfaces obtained after UVO treatment using a hexagonal mask at three different times 10 min, 30 min, and 60 min. Center: Cross-sectional profiles of the patterned surfaces upon UVO exposure times varying from 10 to 60 min. Right: Step induced in the PDMS films as a function of the duration of the UVO treatment. [Color figure can be viewed in the online issue, which is available at wileyonlinelibrary.com.]

top layer the UVO treatment continues further penetrating into the PDMS.

The possibility to generate a surface pattern by surface degradation and simultaneous formation of a rigid SiO_x layer was employed to form structures with three discrete levels of structuration. First, the pattern originated by the mask employed (squares, hexagonal features among others). Moreover, two distinct regions (as has been evidenced above) exposed to UVO during two different periods of time will afford wrinkles with different sizes. Figure 6 (b) and 6(c) shows the SEM images of the surface structures obtained for PDMS films stretched up to 20% and exposed to 40 min with the mask and 20 additional minutes upon mask removal. In these series of images we can observe the pattern induced by degradation of the areas exposed during 1 h (40 + 20 min). These areas form wrinkles with average wavelengths of 1-1.2 μm independently of the mask employed. Those surface regions protected during the first UVO exposure, i.e., those that have been only treated during 20 min also exhibit wrinkles but with a significantly smaller wavelengths below 1 μm (600–800 nm).

CONCLUSIONS

Herein we described the formation of hierarchical wrinkled surfaces obtained by sequential UVO treatments. By positioning a mask on top of the stretched PDMS film allowed us to fine tune the areas exposed and those non-exposed to ozone. Moreover, a second UVO treatment without the mask was required to obtain the wrinkle formation. As a result, wrinkles with different dimensions were obtained depending on the structure of the mask employed.

UVO treatment has been chosen due to their capability to simultaneously rigidify the interface by formation of a SiO_x layer and degrade the surface for longer treatments. By taking into account these two simultaneously occurring processes we were able to induce an additional level of order in these wrinkled films. These are: the structure provided by the mask employed (squares, lines, hexagons, ...), the wrinkled surface inside of the directly exposed areas (related to the hole size of the mask) and the wrinkled surface protected during the first treatment by the mask (which is related to the mesh dimensions of the mask employed).

The use of masks with particular features, the role of the treatment duration on the wrinkle dimensions (wavelength and amplitude) and the pattern originated upon degradation permits to obtain a rather large variety of surface patterns by using this strategy.

EXPERIMENTAL

Materials

The PDMS elastomer was prepared by mixing Sylgard 184 (Dow Corning) with a 10 : 1 ratio of resin to curing agent. The films were cured during 6 h at 50°C.

Fabrication of the Wrinkled Surfaces

The generation of microwinkled surfaces has been carried out applying UVO treatment to a pre-stretched PDMS film. The UVO occurs using a low-pressure mercury lamp that emits at two different wavelengths, i.e., 185 and 254nm. The process generates simultaneously atomic oxygen when molecular oxygen is dissociated by 185 nm and ozone by 254 nm ultraviolet wavelengths. The 254 nm UV radiation is absorbed by most hydrocarbons and also by ozone. Therefore, when both UV wavelengths are present atomic oxygen is continuously generated, and ozone is continually formed and destroyed. As a result, using a UVO both near atomically clean surfaces can be achieved in minutes but also can be applied to chemically modify the surface of polymeric materials.

All the crosslinked PDMS films were cut into 1 cm × 5 cm pieces and exposed to a uniaxial stretching of $\varepsilon = 20\%$. The

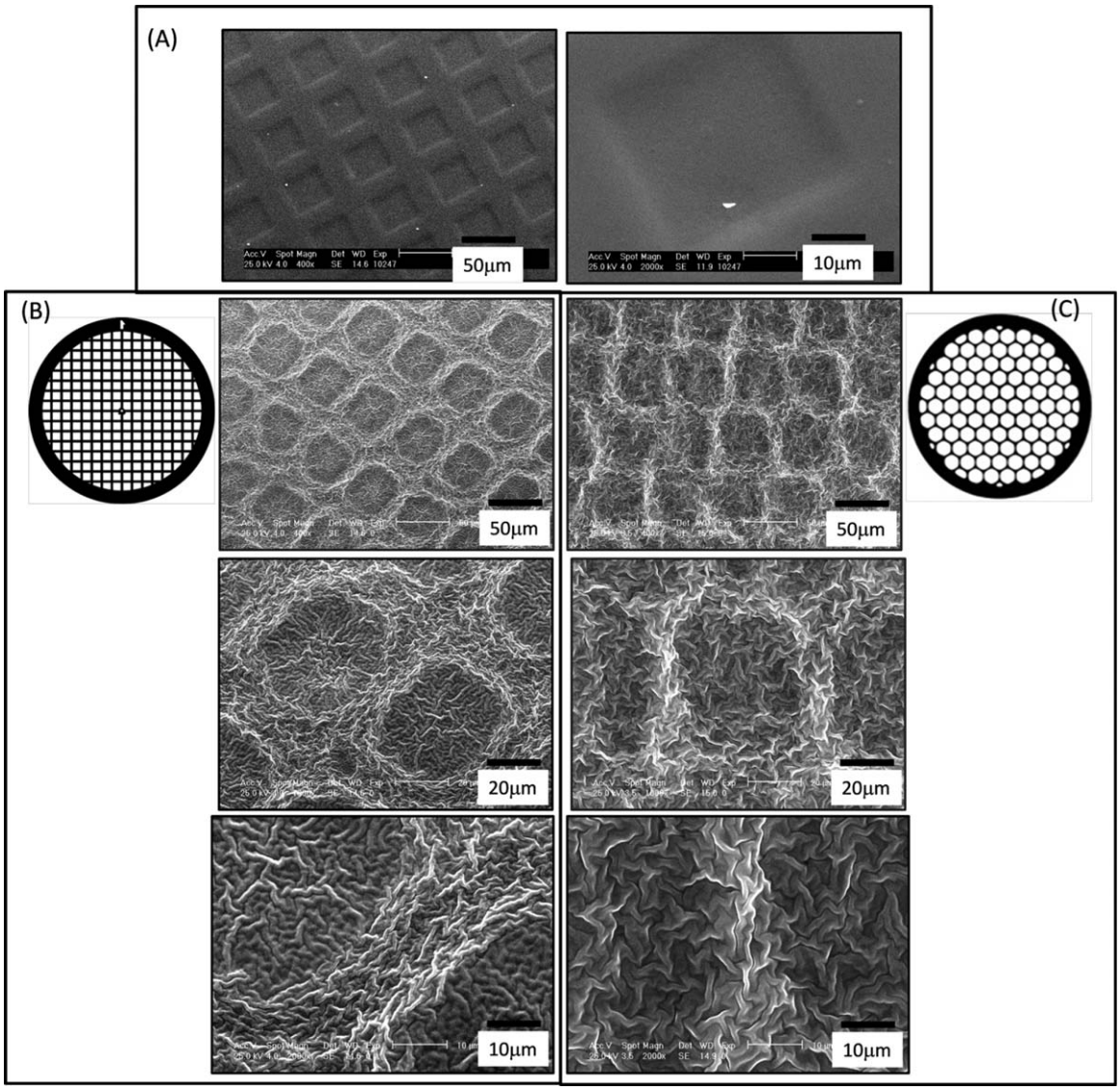

Figure 6. (A) Effect of the UVO treatment on the PDMS surface upon 40 min using a mask. (B) Hierarchically structured wrinkles exhibiting three levels of order: inside of the squares, outside of the squares and the pattern induced by the partial degradation of the PDMS surface. (C) Hierarchically structured pattern similar to (B) but using a hexagonal mask. The treatment employed is composed of two UVO treatment steps: 40 min by using a mask and 20 additional minutes without the mask.

films were mounted into a home-made device to fix the film extremity permitting to apply the desired mechanical deformation. Different masks with variable pattern shapes and sizes were immobilized on top of the stretched films. The oxidation of the PDMS surface with UVO converts the top surface of the PDMS into a rigid silicate-like layer while below the elastic properties remains unchanged. The preparation of wrinkles with variable sizes within the same film required two different treatments to be applied. First, we place a mask on the pre-stretched films and we carried out a UVO treatment so that the areas non-protected by the mask will be exposed. The exposure time of this surface treatment was varied between 0 and 120 min. Then, the mask was removed and an additional surface treatment was applied to rigidity not only the exposed areas but also the areas that were previously protected by the mask. Then the mechanical stretch applied was relaxed and the film was allowed to recover its initial shape. As a result of this relaxation, the oxidized surface and therefore rigidified exhibit an out of plane deformation producing wrinkles with different dimensions depending on the time of exposure applied in each area.

Characterization

Scanning electron microscopy (SEM) micrographs were taken using a Philips XL30 with an acceleration voltage of 25 kV. The samples were coated with gold-palladium (80/20) before scanning. Chemical composition in the different surface areas was determined using confocal Raman microspectroscopy integrated with AFM on a CRM-Alpha 300 RA microscope (WITec, Ulm, Germany) equipped with Nd:YAG dye later (maximum power output of 50 mW power at 532 nm).

Water CA were measured using a KSV Theta goniometer. The volume of the droplets was controlled to be about 2.0 μL and a charge coupled device camera was used to capture the images of the water droplets for the determination of the CA.

Analysis of the degradation as a function of the treatment was carried out with a Zeta-20 optical profiler. This technique permits the 3D visualization of the surface and the analysis of the cross-section profiles.

ACKNOWLEDGMENTS

This work was financially supported by the MINECO (Projects MAT2010-17016 and MAT2010-21088-C03-01).

REFERENCES

1. Lipomi, D. J.; Tee, B. C. K.; Vosgueritchian, M.; Bao, Z. *Adv. Mater.* **2011**, *23*, 1771.
2. Lipomi, D. J.; Lee, J. A.; Vosgueritchian, M.; Tee, B. C. K.; Bolander, J. A.; Bao, Z. *Chem. Mater.* **2012**, *24*, 373.
3. Lacour, S. P.; Wagner, S.; Huang, Z. Y.; Suo, Z. *Appl. Phys. Lett.* **2003**, *82*, 2404.
4. Li, T.; Huang, Z. Y.; Suo, Z.; Lacour, S. P.; Wagner, S. *Appl. Phys. Lett.* **2004**, *85*, 3435.
5. Muller, M.; Karg, M.; Fortini, A.; Hellweg, T.; Fery, A. *Nanoscale* **2012**, *4*, 2491.
6. Schweikart, A.; Pazos-Perez, N.; Alvarez-Puebla, R. A.; Fery, A. *Soft Matter* **2011**, *7*, 4093.
7. Lu, C.; Mohwald, H.; Fery, A. *Soft Matter* **2007**, *3*, 1530.
8. Mueller, M.; Tebbe, M.; Andreeva, D. V.; Karg, M.; Alvarez Puebla, R. A.; Pazos Perez, N.; Fery, A. *Langmuir* **2012**, *28*, 9168.
9. Lee, S. G.; Lee, D. Y.; Lim, H. S.; Lee, D. H.; Lee, S.; Cho, K. *Adv. Mater.* **2010**, *22*, 5013.
10. Chan, E. P.; Smith, E. J.; Hayward, R. C.; Crosby, A. J. *Adv. Mater.* **2008**, *20*, 711.
11. Lin, P.-C.; Vajpayee, S.; Jagota, A.; Hui, C.-Y.; Yang, S. *Soft Matter* **2008**, *4*, 1830.
12. Jin, C.; Khare, K.; Vajpayee, S.; Yang, S.; Jagota, A.; Hui, C.-Y. *Soft Matter* **2011**, *7*, 10728.
13. Vandeparre, H.; Léopoldès, J.; Poulard, C.; Desprez, S.; Derue, G.; Gay, C.; Damman, P. *Phys. Rev. Lett.* **2007**, *99*, 188302.
14. Koo, W. H.; Jeong, S. M.; Araoka, F.; Ishikawa, K.; Nishimura, S.; Toyooka, T.; Takezoe, H. *Nat. Photon.* **2010**, *4*, 222.
15. Yoo, P. J. *Electron. Mater. Lett.* **2011**, *7*, 17.
16. Ohzono, T.; Monobe, H.; Shimizu, Y. *Appl. Phys. Exp.* **2008**, 1.
17. Ohzono, T.; Monobe, H.; Yamaguchi, R.; Shimizu, Y.; Yokoyama, H. *Appl. Phys. Lett.* **2009**, 95.
18. Bowden, N.; Huck, W. T. S.; Paul, K. E.; Whitesides, G. M. *Appl. Phys. Lett.* **1999**, *75*, 2557.
19. Chua, D. B. H.; Ng, H. T.; Li, S. F. Y. *Appl. Phys. Lett.* **2000**, *76*, 721.
20. Fu, C.-C.; Grimes, A.; Long, M.; Ferri, C. G. L.; Rich, B. D.; Ghosh, S.; Ghosh, S.; Lee, L. P.; Gopinathan, A.; Khine, M. *Adv. Mater.* **2009**, *21*, 4472.
21. Zhao, X. M.; Xia, Y. N.; Schueller, O. J. A.; Qin, D.; Whitesides, G. M. *Sensor. Actuat. A-Phys.* **1998**, *65*, 209.
22. Zhao, Y.; Huang, W. M.; Fu, Y. Q. *J. Micromechanics Microeng.* **2011**, 21.
23. Huntington, M. D.; Engel, C. J.; Hryn, A. J.; Odom, T. W. *ACS Appl. Mater. Interf.* **2013**, *5*, 6438.
24. Moon, M.-W.; Lee, S. H.; Sun, J.-Y.; Oh, K. H.; Vaziri, A.; Hutchinson, J. W. *Proc. Natl Acad. Sci. USA* **2007**, *104*, 1130.
25. Kim, P.; Abkarian, M.; Stone, H. A. *Nat. Mater.* **2011**, *10*, 952.
26. Verma, A.; Sharma, A.; Kulkarni, G. U. *Small* **2011**, *7*, 758.
27. Gruner, P.; Arlt, M.; Fuhrmann-Lieker, T. *Chemphyschem 14*, 424 **2013**.
28. Lambricht, N.; Pardoen, T.; Yunus, S. *Acta Mater.* **2013**, *61*, 540.
29. Ramanathan, M.; Lokitz, B. S.; Messman, J. M.; Stafford, C. M.; Kilbey, S. M. II *J. Mater. Chem. C* **2013**, *1*, 2097.
30. Wu, Z.; Bouklas, N.; Huang, R. *Int. J. Solids Struct.* **2013**, *50*, 578.
31. Chen, Z.; Kim, Y. Y.; Krishnaswamy, S. *J. Appl. Phys.* **2012**, 112.
32. Chen, Y.-C.; Crosby, A. J. *Soft Matter* **2013**, *9*, 43.
33. Bowden, N.; Brittain, S.; Evans, A. G.; Hutchinson, J. W.; Whitesides, G. M. *Nature* **1998**, *393*, 146.
34. Genzer, J.; Groenewold, J. *Soft Matter* **2006**, *2*, 310.
35. Genzer, J.; Efimenko, K. *Science* **2000**, *290*, 2130.
36. Huck, W. T. S.; Bowden, N.; Onck, P.; Pardoen, T.; Hutchinson, J. W.; Whitesides, G. M. *Langmuir* **2000**, *16*, 3497.
37. Noorduin, W. L.; Grinthal, A.; Mahadevan, L.; Aizenberg, J. *Science* **2013**, *340*, 832.
38. Mahadevan, L.; Rica, S. *Science* **2005**, *307*, 1740.
39. Yang, S.; Khare, K.; Lin, P.-C. *Adv. Funct. Mater.* **2010**, *20*, 2550.
40. Guo, C. F.; Nayyar, V.; Zhang, Z.; Chen, Y.; Miao, J.; Huang, R.; Liu, Q. *Adv. Mater.* **2012**, *24*, 3010.
41. Watanabe, M. *Soft Matter* **2012**, *8*, 1563.
42. Yoo, P. J.; Suh, K. Y.; Park, S. Y.; Lee, H. H. *Adv. Mater.* **2002**, *14*, 1383.
43. Efimenko, K.; Rackaitis, M.; Manias, E.; Vaziri, A.; Mahadevan, L.; Genzer, J. *Nat. Mater.* **2005**, *4*, 293.
44. Vandeparre, H.; Gabriele, S.; Brau, F.; Gay, C.; Parker, K. K.; Damman, P. *Soft Matter* **2010**, *6*, 5751.
45. Kim, Y. H.; Lee, Y. M.; Lee, J. Y.; Ko, M. J.; Yoo, P. J. *ACS Nano* **2012**, *6*, 1082.
46. Lee, J.-H.; Ro, H. W.; Huang, R.; Lemaillet, P.; Germer, T. A.; Soles, C. L.; Stafford, C. M. *Nano Lett.* **2012**, *12*, 5995.
47. Yin, J.; Lu, C. *Soft Matter* **2012**, *8*, 6528.
48. Ouyang, M.; Yuan, C.; Muisener, R. J.; Boulares, A.; Koberstein, J. T. *Chem. Mater.* **2000**, *12*, 1591.

49. Efimenko, K.; Wallace, W. E.; Genzer, J. *J. Colloid Interface Sci.* **2002**, *254*, 306.
50. Hillborg, H.; Tomczak, N.; Olah, A.; Schonherr, H.; Vancso, G. J. *Langmuir* **2004**, *20*, 785.
51. Olah, A.; Hillborg, H.; Vancso, G. J. *Appl. Surf. Sci.* **2005**, *239*, 410.
52. Diaz-Quijada, G. A.; Peytavi, R.; Nantel, A.; Roy, E.; Bergeron, M. G.; Dumoulin, M. M.; Veres, T. *Lab Chip* **2007**, *7*, 856.
53. Mitchell, S. A.; Poulsson, A. H. C.; Davidson, M. R.; Bradley, R. H. *Colloid Surf. B: Biointerf.* **2005**, *46*, 108.
54. Oláh, A.; Hillborg, H.; Vancso, G. J. *Appl. Surf. Sci.* **2005**, *239*, 410.